

**A REPORT**  
**ON**  
**DEVELOPMENT OF SOFTWARE TOOL**  
**FOR BATHYMETRY MAPPING USING SATELLITE IMAGERY**

**BY**

<b>NAMES</b>	<b>ID NOS.</b>
<b>1. NALLA VENKAT SIDDARTHA REDDY</b>	<b>2016A7PS0030P</b>
<b>2. BHAVESH RANJIT CHAND</b>	<b>2016B5A70715P</b>

**AT**



**INDIAN INSTITUTE OF REMOTE SENSING, DEHRADUN**  
**A PRACTICE SCHOOL-I STATION OF**



**BIRLA INSTITUTE OF TECHNOLOGY AND SCIENCE, PILANI**  
**(JULY, 2018)**

**A REPORT**  
**ON**  
**DEVELOPMENT OF SOFTWARE TOOL**  
**FOR BATHYMETRY MAPPING USING SATELLITE IMAGERY**

**BY**

<b>NAMES</b>	<b>ID NOS.</b>	<b>DISCIPLINES</b>
1. Nalla Venkat Siddartha Reddy	2016A7PS0030P	Computer Science
2. Bhavesh Chand	2016A7PS0013P	Physics & Computer Science

**PREPARED IN PARTIAL FULFILLMENT OF THE**  
**PRACTICE SCHOOL-I COURSE NO. BITS F221**

**AT**



**INDIAN INSTITUTE OF REMOTE SENSING, DEHRADUN**

**A PRACTICE SCHOOL-I STATION OF**



**BIRLA INSTITUTE OF TECHNOLOGY AND SCIENCE, PILANI**  
**(JULY, 2018)**

## **ACKNOWLEDGEMENTS**

The entire Practice School experience, has been a great learning experience. To all the people who made that possible, we extend our sincere gratitude and appreciation.

Firstly, we thank Dr. Prakash Chauhan, Director of IIRS, Dehradun for giving us this wonderful opportunity and providing us with all the necessary facilities.

We are also thankful to Mrs. Shefali Agarwal, Group Head of Geospatial Technology and Outreach Programme, IIRS, for her valuable support.

We extend our most sincere gratitude to Dr. Debashis Mitra, Group Head of Marine & Atmospheric Sciences Department, IIRS, for providing us with the opportunity to work on this project and for his valuable guidance at each and every step throughout.

In addition, we wish to extend our gratitude to our PS Instructor, Dr. Chandra Shekhar, Associate Professor at BITS, Pilani – Pilani Campus, for his guidance, advice and support as and when needed.



# **TABLE OF CONTENTS**

i.	Title page .....	1
ii.	Acknowledgements .....	2
iii.	Abstract Sheet .....	3
<hr/>		
1.	Introduction .....	6
1.1.	Remote Sensing .....	6
1.2.	Bathymetry .....	7
1.2.1.	Need for Satellite Bathymetry .....	8
2.	Separation of land and sea .....	9
3.	Water Column Correction .....	10
3.1.	When to implement Water Column Correction .....	11
3.1.1.	Multispectral classification of marine habitats .....	11
3.1.2.	Establishing empirical relationships between image and marine features ....	11
3.1.3.	Visual interpretation of digital data .....	11
3.2.	Lyzenga's Algorithm .....	11
3.2.1.	Atmospheric Correction .....	12
3.2.2.	Linearise relationship between Depth and Radiance .....	12
3.2.3.	Attenuation Coefficient .....	12
3.2.4.	Depth invariant Index of bottom type .....	13
4.	Depth .....	15
4.1	Georeferencing survey map .....	15
4.2	Picking Ground Truth points .....	15
4.3	Obtaining Green radiance values and calculating regression .....	15
4.4	Validation of obtained depth with sample depths .....	16
5.	Python Libraries used .....	17
5.1.	PyQt4 .....	17
5.2.	NumPy .....	17

5.3. Rasterio .....	17
5.4. Matplotlib .....	18
5.5. UTM .....	18
6. Graphical User Interface(GUI) .....	18
6.1. For Water column correction .....	20
6.2. For Depth Processing .....	21
6.3. For Points file .....	22
7. Datasets Used .....	23
7.1. Adding Flexibility .....	23
8. Results .....	23
9. Recommendations .....	26
10. Appendices .....	26
10.1. Appendix-I: Calculation of Ratio of Attenuation Constants .....	27
10.2. Appendix-II: Band notations of LandSat satellites .....	28
11. References .....	30
12. Glossary .....	30

# 1. INTRODUCTION

## 1.1 Remote Sensing

Remote sensing is the acquisition of information about an object or phenomenon without making physical contact with the object and thus in contrast to on-site observation. Remote sensing is used in numerous fields, including geography, land surveying and most Earth Science disciplines (for example, hydrology, ecology, oceanography, glaciology, geology); it also has military, intelligence, commercial, economic, planning, and humanitarian applications. In current usage, the term "remote sensing" generally refers to the use of satellite- or aircraft-based sensor technologies to detect and classify objects on Earth, including on the surface and in the atmosphere and oceans, based on propagated signals (e.g. electromagnetic radiation). It may be split into "active" remote sensing (i.e., when a signal is emitted by a satellite or aircraft and its reflection by the object is detected by the sensor) and "passive" remote sensing (i.e., when the reflection of sunlight is detected by the sensor).

Remote sensing makes it possible to collect data of dangerous or inaccessible areas. Remote sensing applications include monitoring deforestation in areas such as the Amazon Basin, glacial features in Arctic and Antarctic regions, and depth sounding of coastal and ocean depths.

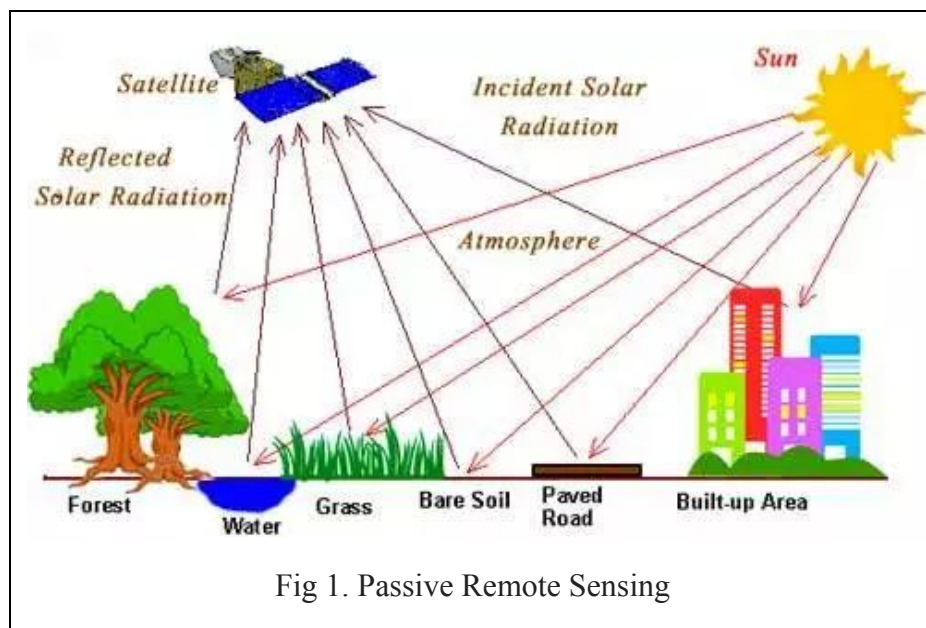
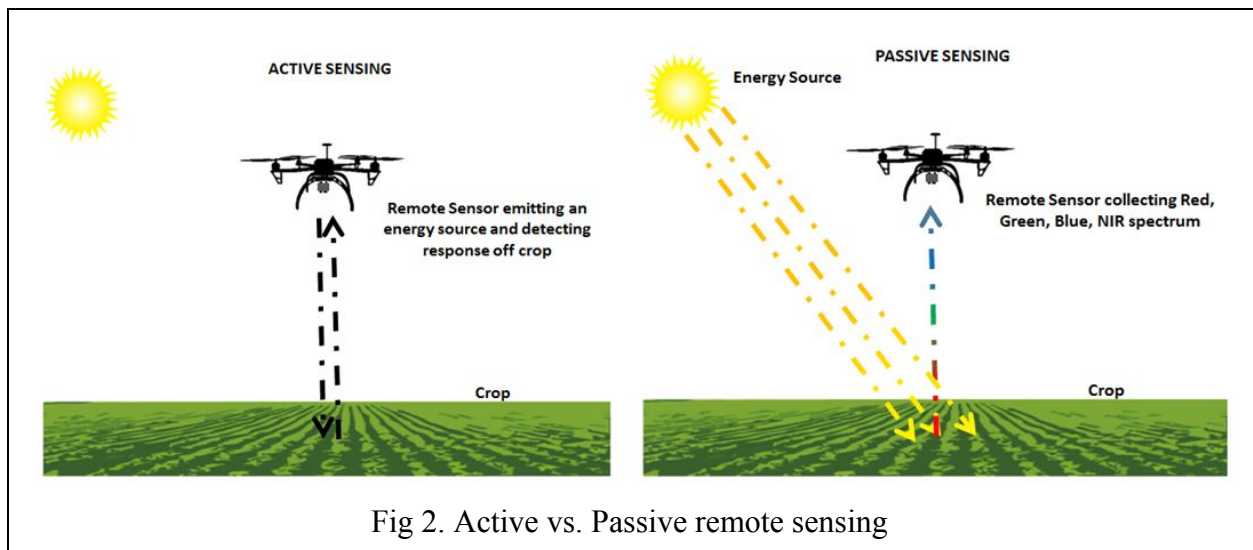


Fig 1. Passive Remote Sensing

Military during the Cold War made use of remote sensing for collection of data about dangerous border areas. Remote sensing also replaces costly and slow data collection on the ground, ensuring in the process that areas or objects are not disturbed.

Orbital platforms collect and transmit data from different parts of the electromagnetic spectrum, which in conjunction with larger scale aerial or ground-based sensing and analysis, provides researchers with enough information to monitor trends such as El Niño and other natural long and short term phenomena. Other uses include different areas of the earth sciences such as natural resource management, agricultural fields such as land usage and conservation, and national security and overhead, ground-based and stand-off collection on border areas.



## 1.2 Bathymetry

Bathymetry is the study of underwater depth of lake or ocean floors. Bathymetric charts are typically produced to support safety of surface or subsurface navigation, and usually show seafloor relief or terrain as contour lines and selected depths, and typically also provide surface navigational information. Bathymetric maps may also use a Digital Terrain Model and artificial illumination techniques to illustrate the depths being portrayed.

### 1.2.1 Need for Satellite Bathymetry

After five decades of surveying by ships carrying echosounders, most of the ocean floor remains unexplored and there are vast gaps between survey lines. The primary reason for this lack of data is that ships are slow and expensive to operate. The chief advantage of satellites is their relatively higher speed and lower cost. A systematic survey of the oceans by ships would take more than 200 years of survey time at a cost of billions of U.S. dollars. A complete satellite survey can be made in five years for under \$100M.

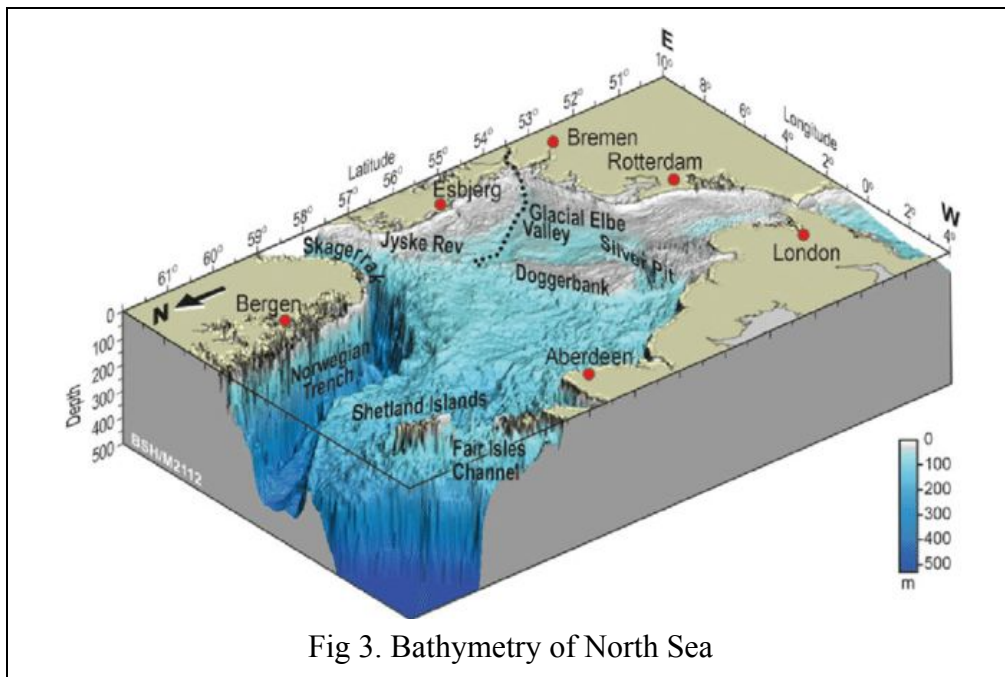


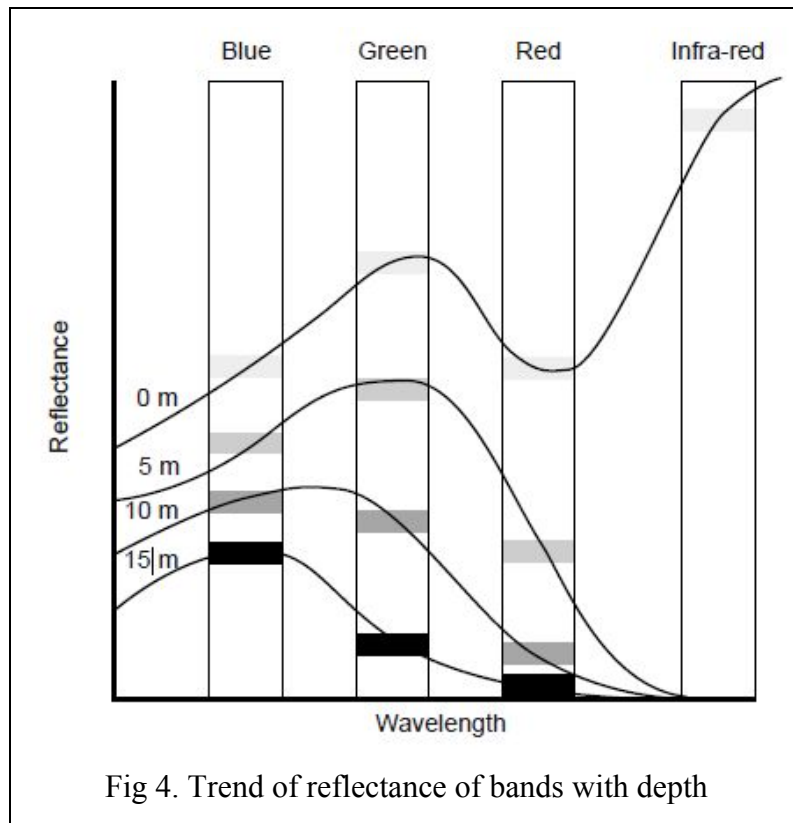
Fig 3. Bathymetry of North Sea

Satellites have another advantage in comparison to the present database of echo soundings, namely globally uniform resolution. By carrying the same sensor all over the globe, a satellite makes measurements of the same quality everywhere, a requirement for mapping the global distribution patterns of small bathymetric features. Ships have not done this. The era of frontier exploration, when scientists could take ships into remote areas merely for curiosity's sake, was an era of single-beam echo sounders and relatively poor navigation. The last two decades have seen great technical advances in echo sounding and navigation (Global Positioning System), but these have been deployed over only a few percent of the ocean's area. The focus has been on coastal regions and Exclusive Economic Zones, and research emphasizing

“hypothesis testing,” which requires ships to revisit previously surveyed areas. The result is that even today, most of the data available in the remote oceans are the old-style, low-tech data.

A third advantage of satellites is that they can go everywhere, without making noise. Some countries prevent ships from surveying in their territorial waters. Concerns have been raised recently that the use of acoustic devices may harm marine life, and it is now becoming more difficult to get permission to use acoustic systems. These concerns may ultimately make global surveys by ships impossible.

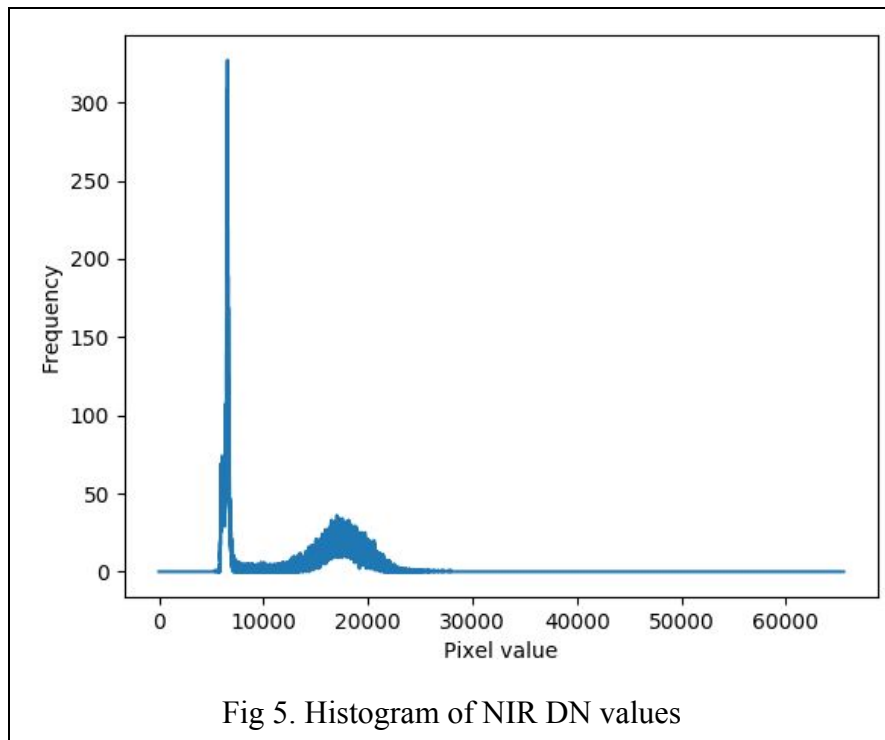
## 2. Separation of land and water



Penetrative power of light decreases with increase in wavelength. Especially so in water, the Near Infrared band fails to penetrate even a few centimeters deep due to very strong absorption. Moreover, NIR radiation is characteristically very strongly reflected by vegetation

and soil. As a result, a stark difference can be visually observed between land and water bodies in NIR band images and there is a drastic difference in the DN values as well.

If we plot a histogram of NIR band DN values, 2 peaks can be observed, the first one of which is the collection of water pixels and the second one a collection of land pixels. On visual inspection, the user has to click on the histogram so as to select a threshold value somewhere between these peaks. The option of manually feeding this value has also been provided. This threshold value is then used to mask out points which correspond to land so that we get an array of water body pixels only to run further processing on.



### **3. Water Column Correction**

When light penetrates water its intensity decreases exponentially with increasing depth. This process is known as attenuation and it exerts a profound effect on remotely sensed data of aquatic environments. The severity of attenuation differs with the wavelength of electromagnetic radiation (EMR). In the region of visible light, the red part of the spectrum attenuates more rapidly than the shorter-wavelength blue part. As depth increases, the separability of habitat spectra declines. In practice, the spectra of sand at a depth of 2 m will be very different to that at

20 m – yet the substratum is the same. In fact, the spectral signature of sand at 20 m may be similar to that of seagrass at (say) 3 m. The spectral radiances recorded by a sensor are therefore dependent both on the reflectance of the substrata and on depth. These two influences on the signal will create considerable confusion when attempting to use visual inspection or multispectral classification to map habitats. Since most marine habitat mapping exercises are only concerned with mapping benthic features, it is useful to remove the confounding influence of variable water depth. The algorithm implemented is only truly applicable to clear waters such as those in coral reef environments.

### **3.1 When to implement Water Column Correction**

#### **3.1.1 Multispectral classification of marine habitats**

The accuracies of some habitat maps of the Turks and Caicos Islands showed significant improvement once water column correction had taken place. Improvements to accuracy were greatest for imagery which had at least three water-penetrating spectral bands, from which three (or more) depth-invariant bottom indices could be created and input to the spectral classification.

#### **3.1.2 Establishing empirical relationships between image and marine features**

Water column correction was found to be essential for relating digital image data to seagrass standing crop.

#### **3.1.3 Visual interpretation of digital data**

By removing much of the depth-induced variation in spectral data, water column correction makes for a better visual assessment of habitat types.

### **3.2 Lyzenga's Algorithm**

Removal of the influence of depth on bottom reflectance would require:

- A measurement of depth for every pixel in the image
- A knowledge of the attenuation characteristics of the water column

Good digital elevation models of depth are rare, particularly for coral reef systems where charts are often inaccurate. As a compromise, Lyzenga (1978, 1981) put forward a simple image-based approach to compensate for the effect of variable depth when mapping bottom features. Rather than predicting the reflectance of the seabed, which is prohibitively difficult, the method produces a ‘depth-invariant bottom index’ from each pair of spectral bands.

### **3.2.1 Atmospheric Correction**

It is the removal of scattering in the atmosphere and external reflection from water surface. This is based on the ‘dark pixel subtraction’ method. A large number of pixels are sampled from ‘deep water’ and their average radiance is then subtracted from all other pixels in each band respectively:

$$\textit{Atmospherically corrected radiance} = L_i - L_{si}$$

where  $L_i$  is the pixel radiance in band  $i$  and  $L_{si}$  is the average radiance for deep water in band  $i$ .

### **3.2.2 Linearise relationship between Depth and Radiance**

In relatively clear water, the intensity of light will decay exponentially with increasing depth. If values of light intensity (radiance) are transformed using natural logarithms (ln), this relationship with depth becomes linear. Transformed radiance values will therefore decrease linearly with increasing depth. If  $X_i$  is the transformed radiance of a pixel in band  $i$ , this step is written as:

$$X_i = \ln(L_i - L_{si})$$

### **3.2.3 Attenuation Coefficient**

The irradiance diffuse attenuation coefficient (hereafter referred to as attenuation coefficient,  $k$ ) describes the severity of light attenuation in water for that spectral band. It is related to radiance and depth by the following equation where  $a$  is a constant,  $r$  is the reflectance of the bottom and  $z$  is depth:

$$L_i = L_{si} + a.r.e^{-2kiz}$$

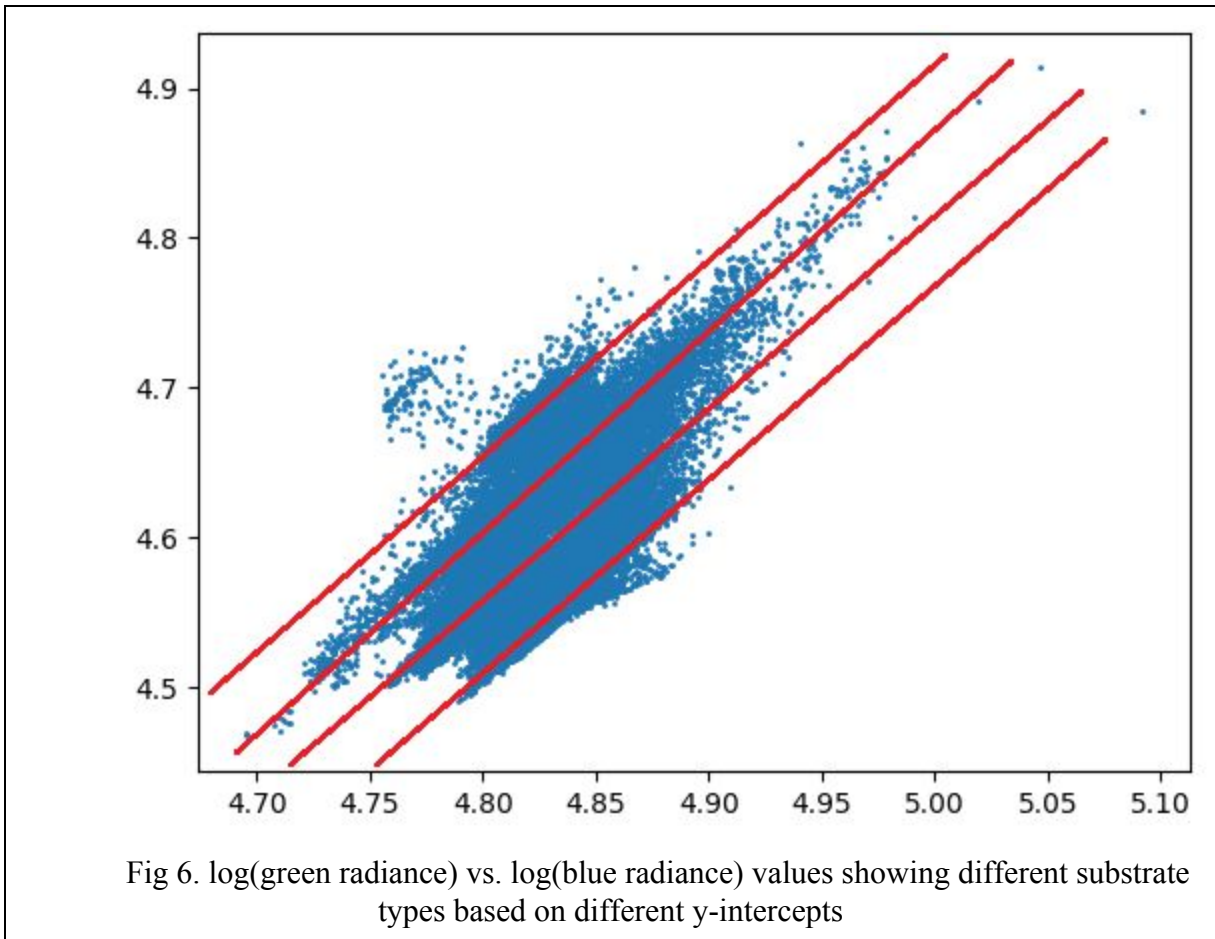
Theoretically, it would be possible to rearrange the equation and generate an image of bottom type,  $r$  (reflectance) which is the measurement we seek. However, this approach is not feasible because there are too many unknown quantities – i.e. the value of the constant  $a$ , the attenuation coefficient for each band and the depth of water at each pixel. The method developed by Lyzenga does not require the actual calculation of these parameters but gets around the problem by using information from more than one band. All that is required is the ratio of attenuation coefficients between pairs of spectral bands. Use of ratios cancels out many of these unknowns and the ratios can be determined from the imagery itself.

#### **3.2.4 Depth invariant Index of bottom type**

If radiance (reflectance) values for another bottom type were added to the bi-plot, a similar line would be obtained – once again, the only change between data points would be depth. However, since the second bottom type will not have the same reflectance as the first, the new line will be displaced either above or below the existing line (e.g. if line 1 was derived from sand which generally has a high reflectance, and line 2 was generated from seagrass with lower reflectance, the latter line would lie below that for sand). The gradient of each line should be identical because the ratio of attenuation coefficients  $k_i / k_j$  is only dependent on the wavelength of the bands and clarity of the water.

An index of bottom type can be obtained by noting the y-intercept for each bottom type. For example, while pixel values lying on the line for sand show considerable variation in radiance, they all represent the same bottom type and have the same y-intercept. The y-intercept for pixels of seagrass is considerably different. The y-axis therefore becomes an axis (or index) of bottom type. Of course, not all pixel values for a given bottom type lie along a perfectly straight line. This is because of natural variation in bottom reflectance, patches of turbid water and sensor noise. Nevertheless, each pixel can be assigned an index of bottom type once the ratio of attenuation coefficients has been estimated ( $k_i / k_j$ ). This is accomplished by ‘connecting’ each pixel on the bi-plot to the y-axis using an imaginary line of gradient  $k_i / k_j$ . Pixel values on the bi-plot are then converted to their corresponding positions on the y-axis (index of bottom type). Using this method, each pixel value is converted to an index of bottom type, which is

independent of depth. These depth-invariant indices of bottom type lie along a continuum but pixels from similar habitats will have similar indices.



The mathematics of the depth-invariant index are simple and are based on the equation of a straight line:

$$y = p + q \cdot x$$

where p is the y-intercept, q is the gradient of the regression of y on x.

The equation can be rearranged to give the y-intercept:

$$p = y - q \cdot x$$

which becomes,

$$\text{depth invariant index} = \ln(L_i - L_{si}) - \left[\left(\frac{k_i}{k_j}\right) \cdot \ln(L_j - L_{sj})\right]$$

Each pair of spectral bands will produce a single depth-invariant band of bottom type. If the imagery has several bands with good water penetration properties, multiple depth-invariant bands can be created. The depth-invariant bands may then be used for image processing or visual inspection instead of the original bands.

We are using blue and green bands because these 2 bands have the strongest penetration, and thus give output which has the most discernible substrate features.

## **4. Depth Derivation**

### **4.1 Georeferencing survey map**

Hydrographic survey map was obtained from NHO. This is just the scanned copy of chart which is published by the organisation. It is naturally not georeferenced. Georeferencing of this image is required so that we can get proper coordinates of the points used for regression. As this map is not distorted and follows the same Coordinate Projection Datum (WGS-1984) as the satellite imagery, we chose to simply select any 4 points on the map whose coordinates are clearly labelled and georeference it.

Using Open Source Software like QGIS for this purpose is a lot easier and much more functional than writing code for it. So, we georeferenced the map using QGIS.

### **4.2 Picking Ground Truth points**

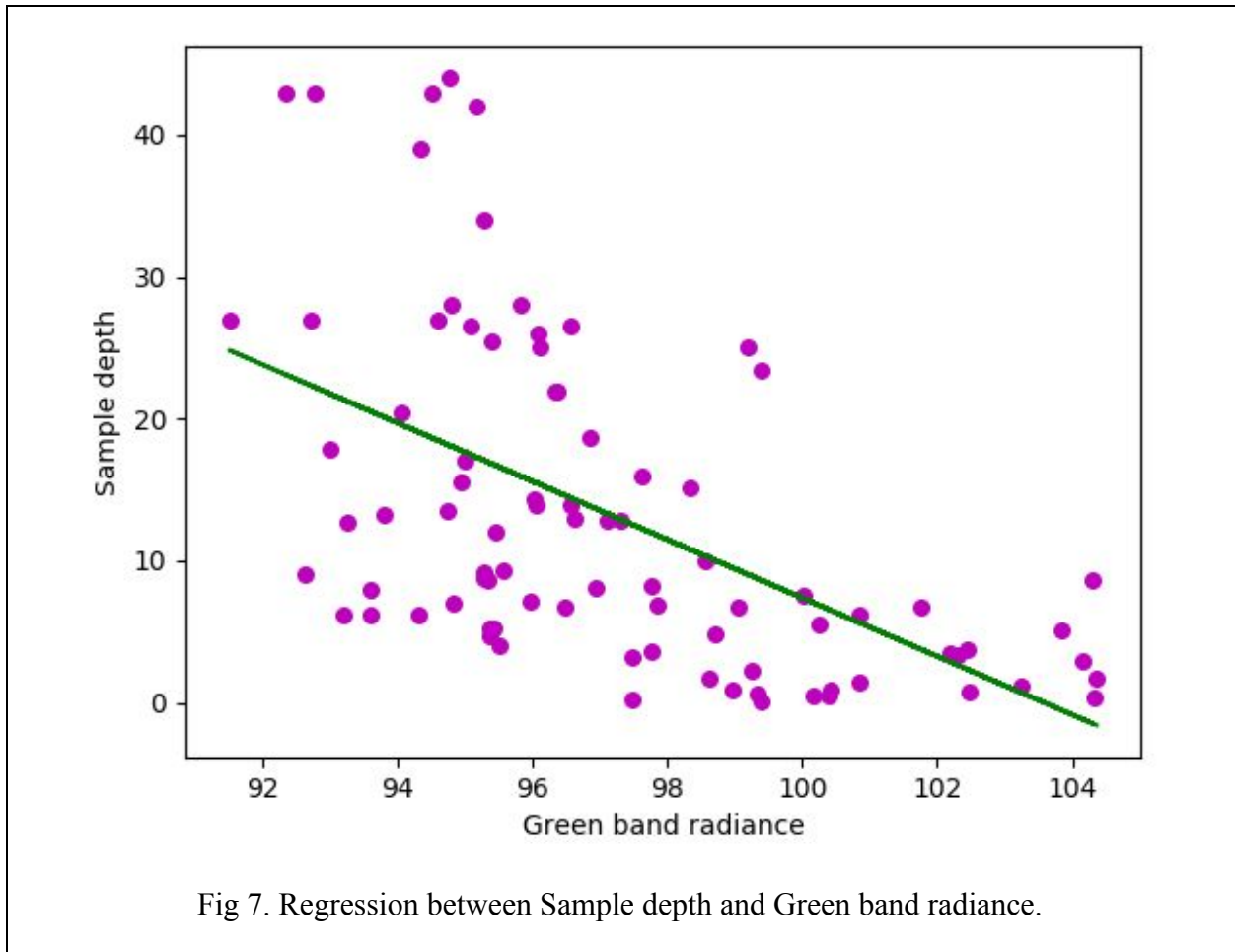
To have ground truth values, user has 2 avenues. First, load georeferenced image and pick at least 50 points within the satellite image area to obtain a good set. Or second, to input a CSV file which contains some points' coordinates and depths. To avoid having to do such toiling work again and again, we have provided a separate program to load the georeferenced map and save CSV file from it which can be reused as many times as the user may want.

### **4.3 Obtaining Green radiance values and calculating regression**

The ground truth values obtained in the previous section have been split in 2 arrays in 3:1 ratio as training and testing data. For the selected points, we are indexing the Green radiance

array with the coordinates to get values at every point. Then, a scatter plot is constructed between the radiance and the training set sample depths to get a regression between them. But, in some sets, in case the area of interest used is so large that it cannot be reasonably assumed that the substrate type is the same, the user will have to select outlier values by mouse click to ignore the other points and get a correct regression.

$$Depth = m * (green\ band\ radiance) + c$$



#### **4.4 Validation of obtained depth with sample depths**

From the training set earlier separated out, we are trying to correlate the depth predicted by regression for these pixels with the sample depths. We are calculating the R\_square value as a measure of correctness of the analysis. R-squared is a statistical measure of how close the data

are to the fitted regression line. It is also known as the coefficient of determination, or the coefficient of multiple determination for multiple regression.

R-squared is always between 0 and 1. 0 indicates that the model explains none of the variability of the response data around its mean. 1 indicates that the model explains all the variability of the response data around its mean.

## **5. Python Libraries Used**

### **5.1 PyQt4**

PyQt4 was used to implement the Graphical User Interface for the Python Program. It was used to make 3 windows. The first window being the common window whereas the second window is used for water column correction and the third window is used for depth calculation.

### **5.2 NumPy**

NumPy, which stands for Numerical Python, is a library consisting of multidimensional array objects and a collection of routines for processing those arrays. Using NumPy, mathematical and logical operations on arrays can be performed easily. The pixel data of the images is being stored in NumPy arrays and the final output NumPy array is converted to an image and given as output.

### **5.3 Rasterio**

Rasterio is used to work with satellite image. It was preferred over OpenCV as it preserves the spatial coordinates thus making the output file usable in softwares like QGIS. It is used to read the input images into a NumPy array and convert the final NumPy array into output image.

## **5.4 Matplotlib**

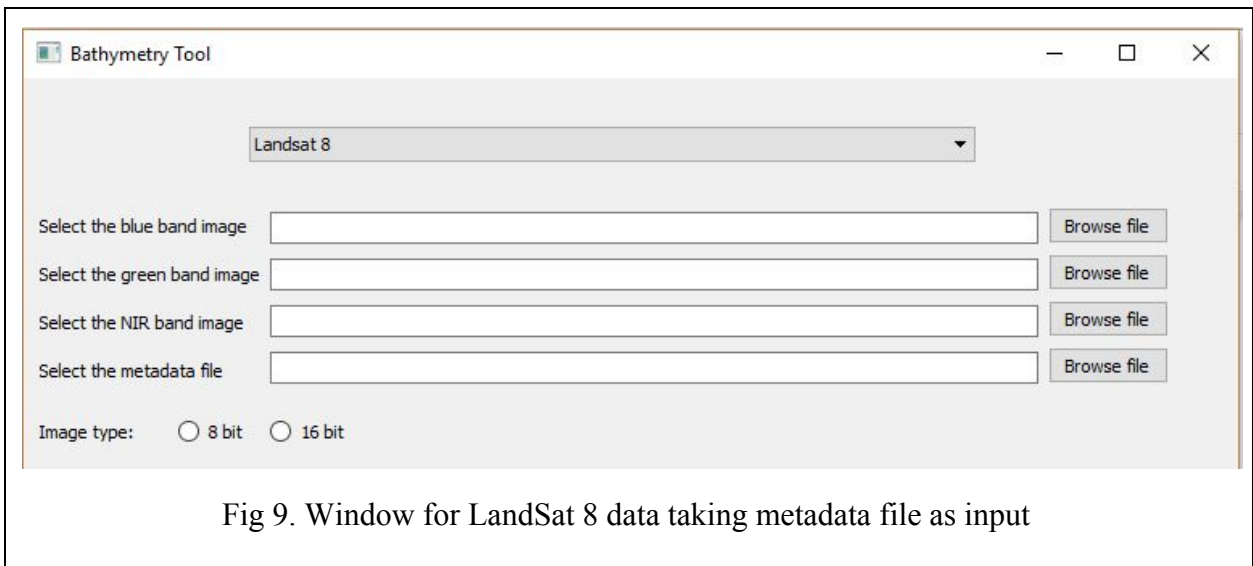
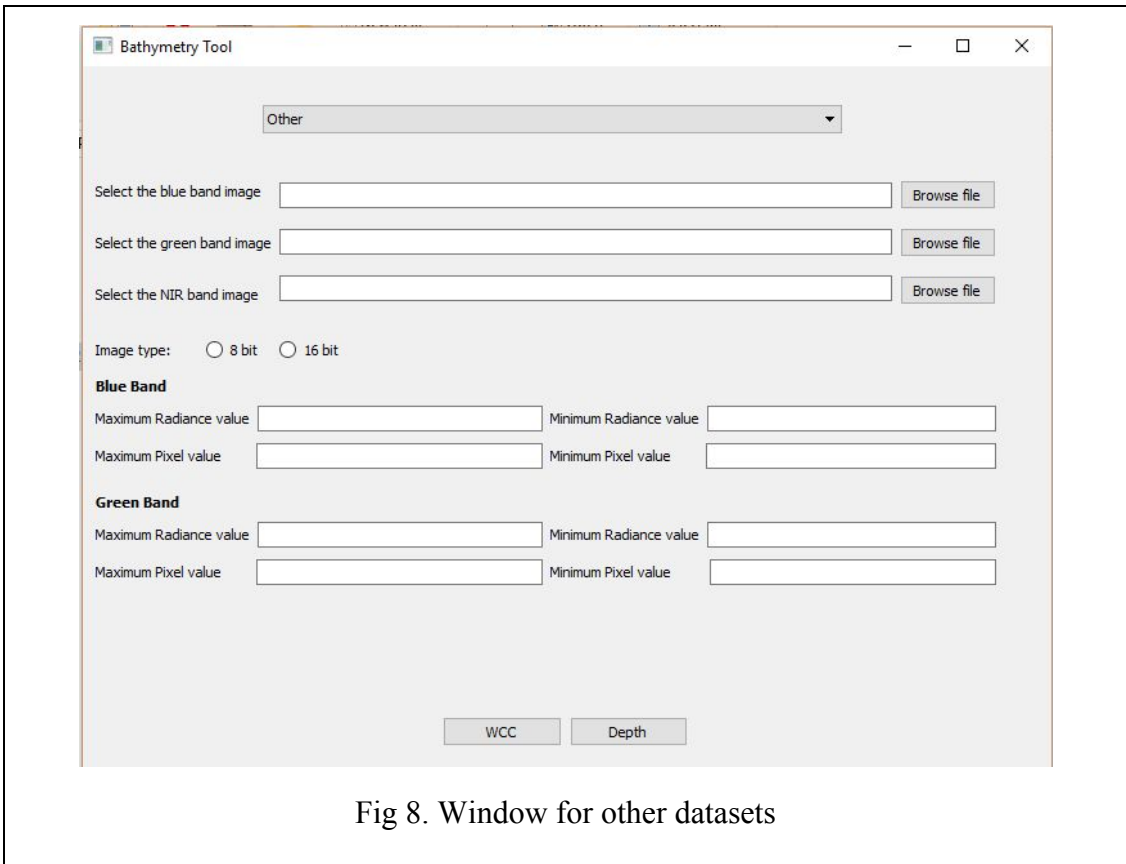
Matplotlib is a Python 2D plotting library which produces publication quality figures in a variety of hardcopy formats and interactive environments across platforms. We are using it to show scatterplots, regression lines and images at multiple points in the processing of the program. All graphs are plotted in matplotlib's interactive API which allows panning, zooming, etc. on the fly. Also, it is being used to dynamically take inputs from user by mouseclicks.

## **5.4 UTM**

Utm is a bidirectional UTM-WGS84 converter for python. We are using it to convert between latitude-longitude to UTM easting-northing when selecting training points.

## **6. Graphical User Interface(GUI)**

The next step was to make a user-friendly GUI. The GUI is made using the PyQt4 library which gives native feel to the GUI and is platform independent. The snippets of the GUI are as shown below. First the user clicks on the executable which opens a window. The user enters the necessary inputs which include blue image file, the green image file, the NIR image file and the datatype. Depending on the dataset varied inputs are required which is explained in the next section. After entering the inputs the user has two options - WCC(water column correction) and depth processing.



## 6.1 For Water Column Correction

Clicking on the WCC button opens a new Window. The first input is the threshold value to separate land and water using histogram if needed. This was elaborated in section 3. The other inputs required are output directory and output filenames. The user can select if he wants to get grayscale image or colour image as output. Grayscale image preserves spatial coordinates and can be used for other purposes on softwares like QGIS. The colour image helps to visualize and understand the output better. Clicking on compute leads to the display of a 'Processing' label which is important as the program takes about a minute to run. After the program has run, a dialog box is shown which indicates that the process is done and the windows close. Along with the image outputs a logfile is also made which contain details that can be used to get the exact values of depth invariant indices. The image has scaled values according to minimum and maximum pixel values.

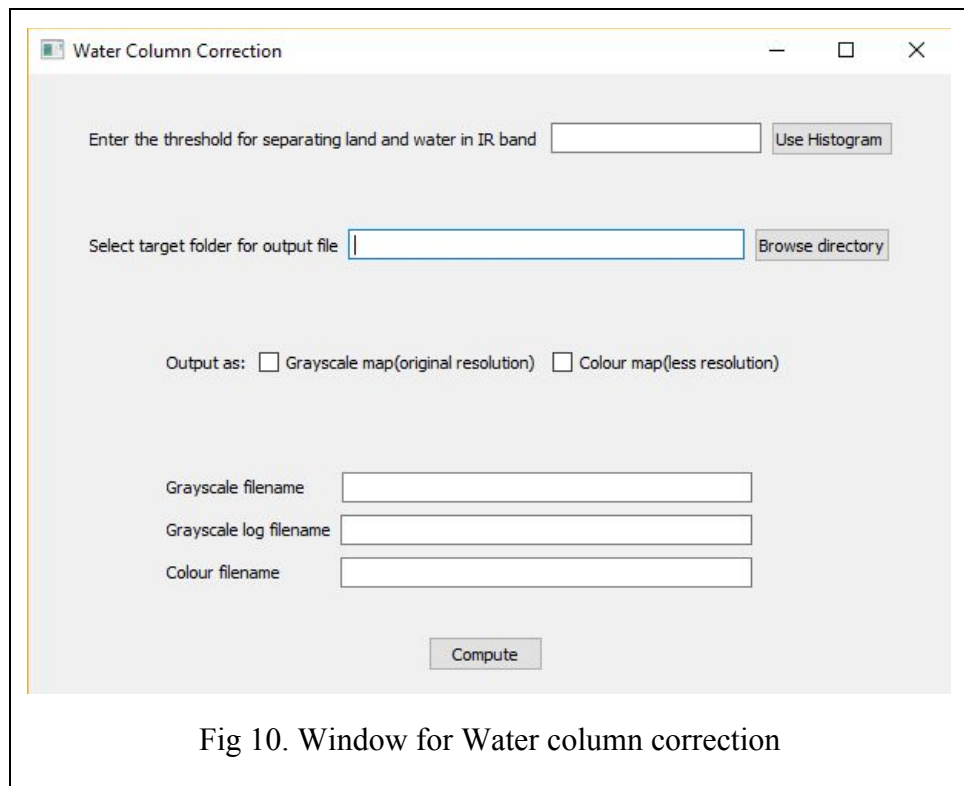
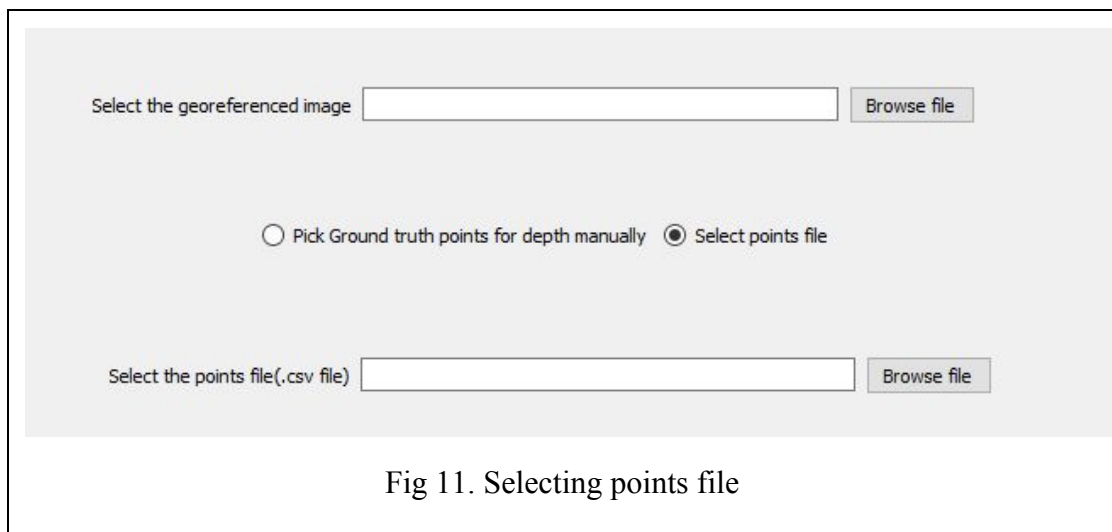


Fig 10. Window for Water column correction

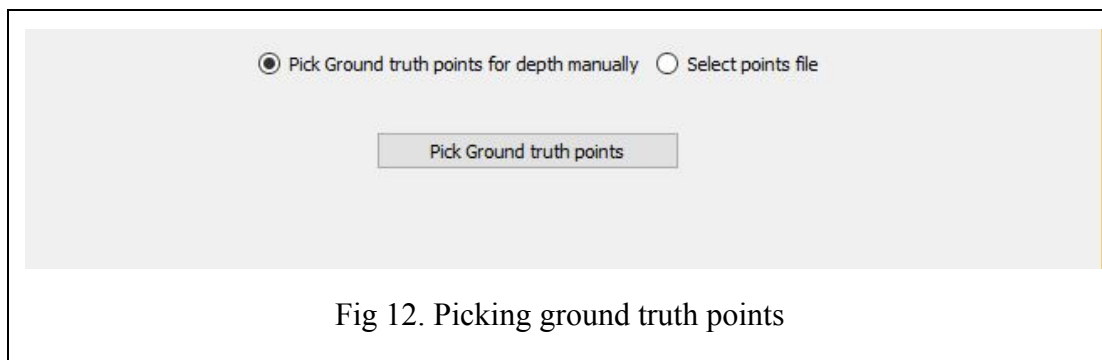
## 6.2 For Depth processing

This window is similar to the WCC window with a few additional inputs. A georeferenced image is needed as input which is a map containing accurate depth values at various coordinates. You can either input a points file having coordinates and depth in a .csv file or you can select ground truth points. The latter option opens the map which can be zoomed in and you can enter depth after clicking a point on the map. Coordinates are recorded by the click and the coordinates and depth values are stored in an array. The output is similar to water column correction. A logfile is also given as output similar to water column correction window.



The screenshot shows a software interface for selecting a points file. It features a text input field labeled "Select the georeferenced image" with a "Browse file" button to its right. Below this, there are two radio buttons: "Pick Ground truth points for depth manually" (which is unselected) and "Select points file" (which is selected). At the bottom, there is another text input field labeled "Select the points file(.csv file)" with a "Browse file" button to its right.

Fig 11. Selecting points file



The screenshot shows the software interface after selecting the "Pick Ground truth points for depth manually" option. The radio button for "Pick Ground truth points for depth manually" is now selected, and the "Select points file" option is unselected. A "Pick Ground truth points" button is centered on the screen.

Fig 12. Picking ground truth points

### 6.3 For Points file

Entering ground truth values repeatedly is a waste of time and hence we have added another executable file. Opening this file will open a window. The window takes georeferenced map, points filename and target directory as input. On clicking the OK button the map opens and you can pick points and enter depth values similar to the depth processing window. The output is a .csv file which can be used as input for depth processing.

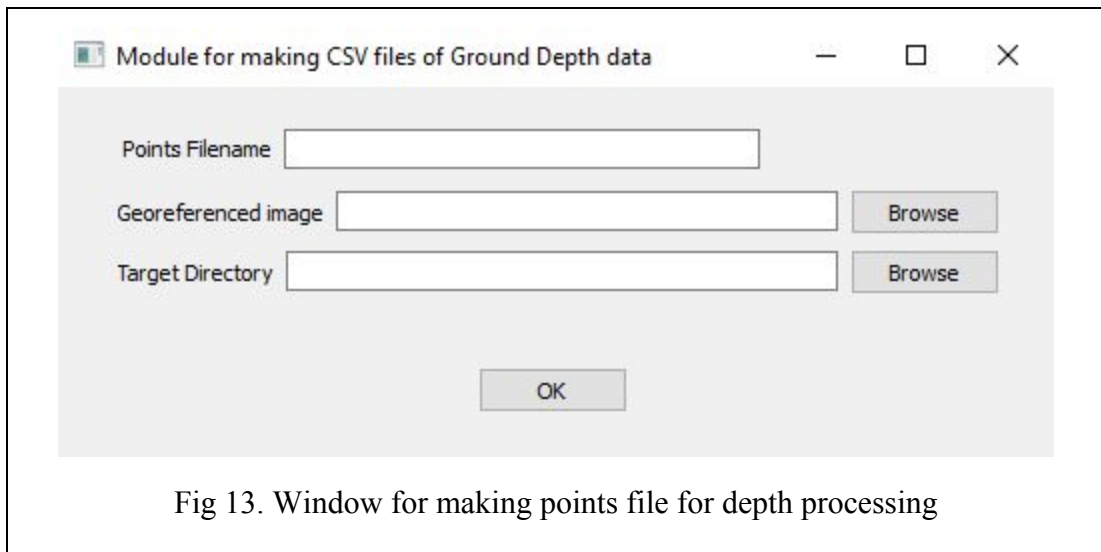


Fig 13. Window for making points file for depth processing

## **7. Datasets Used**

- Cloudless LandSat 8 image of South Andaman obtained from [usgs.glovis.com](https://usgs.glovis.com)
  - Resolution - 30m
- Map of South Andaman having accurate depth measurements (obtained from NHO).

### **7.1 Adding Flexibility**

The code is very flexible, i.e., it can be used for datasets of various satellites. Since Metadata files of images of different satellites vary drastically, we have accounted for only for the following datasets:

- LandSat 5
- LandSat 7
- LandSat 8

For other datasets, the various parameters required for the program are taken directly as input from the user without taking metadata file.

All the datasets that can be read by rasterio can be used as input given that the images are georeferenced.

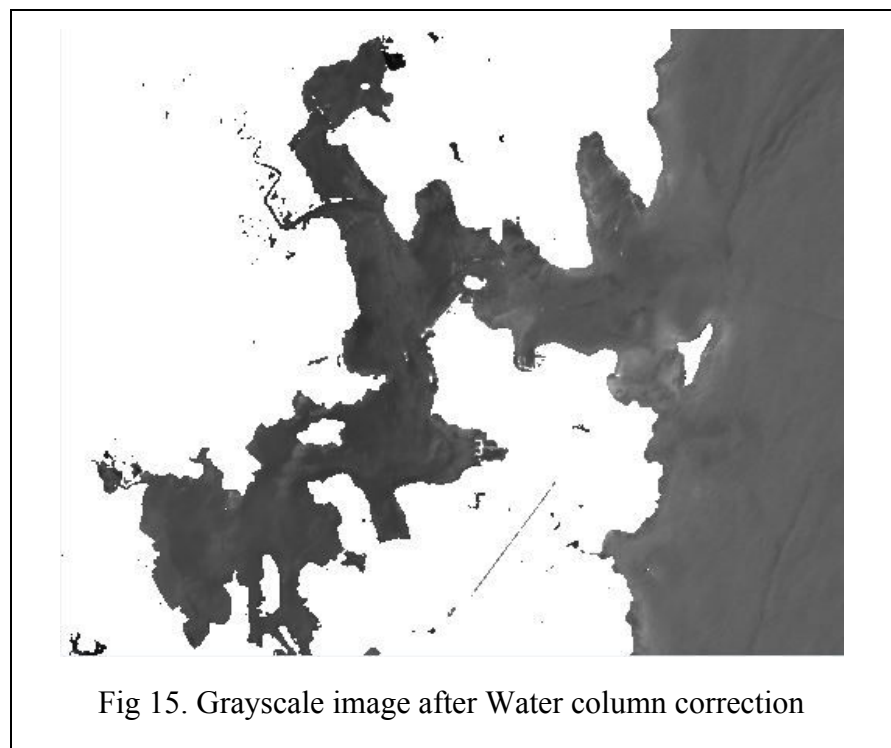
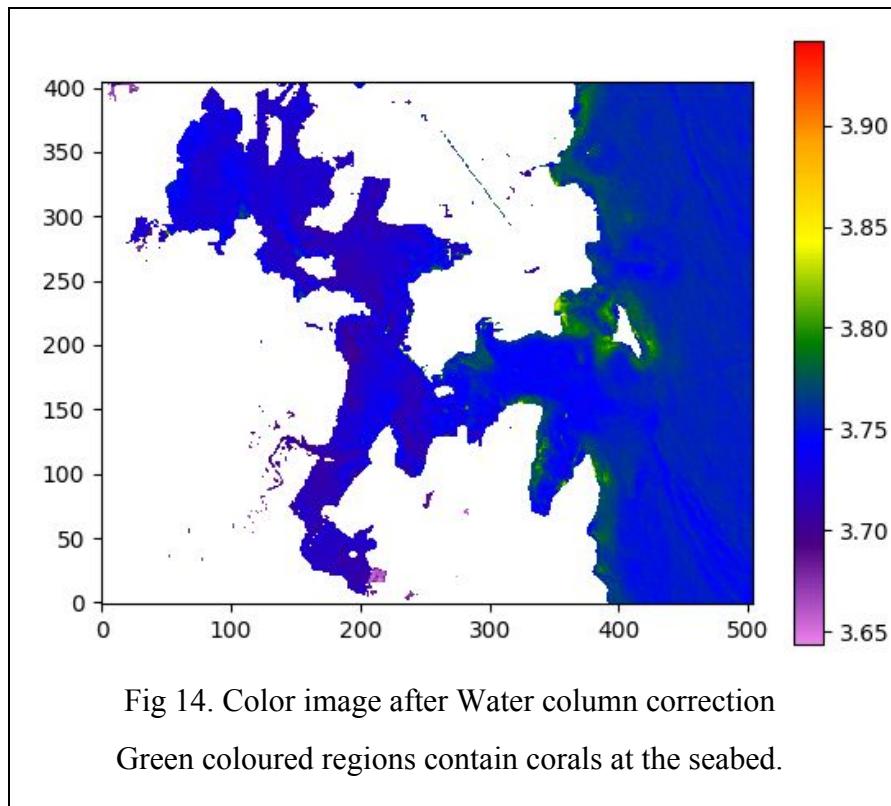
## **8. Results**

The tool aims to create bathymetry maps of depth-invariant indices and depth according to what the user needs.

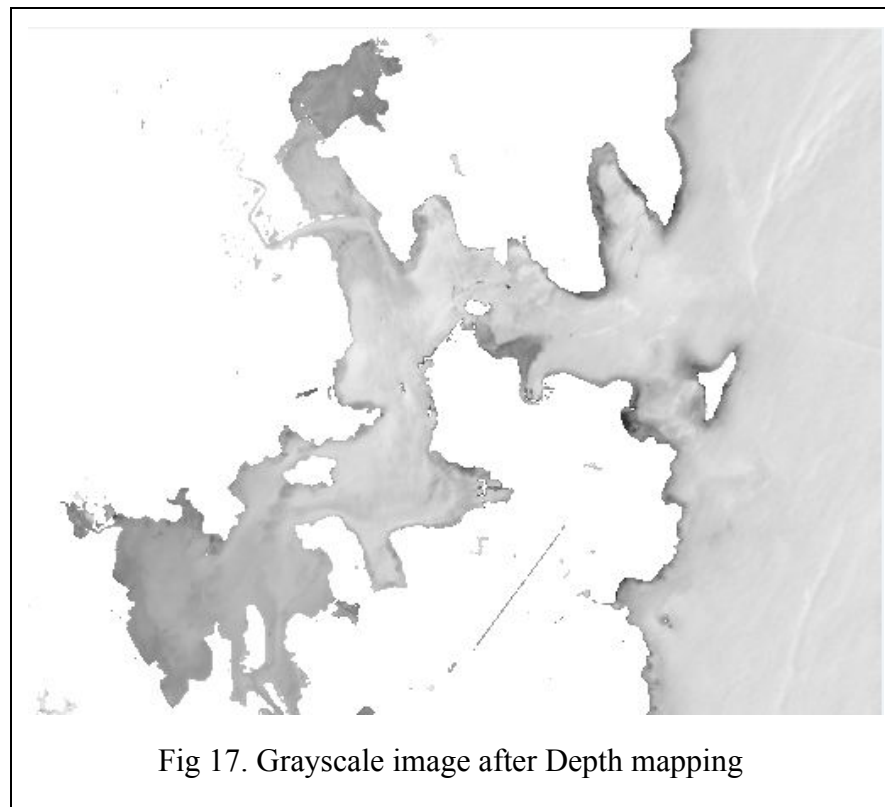
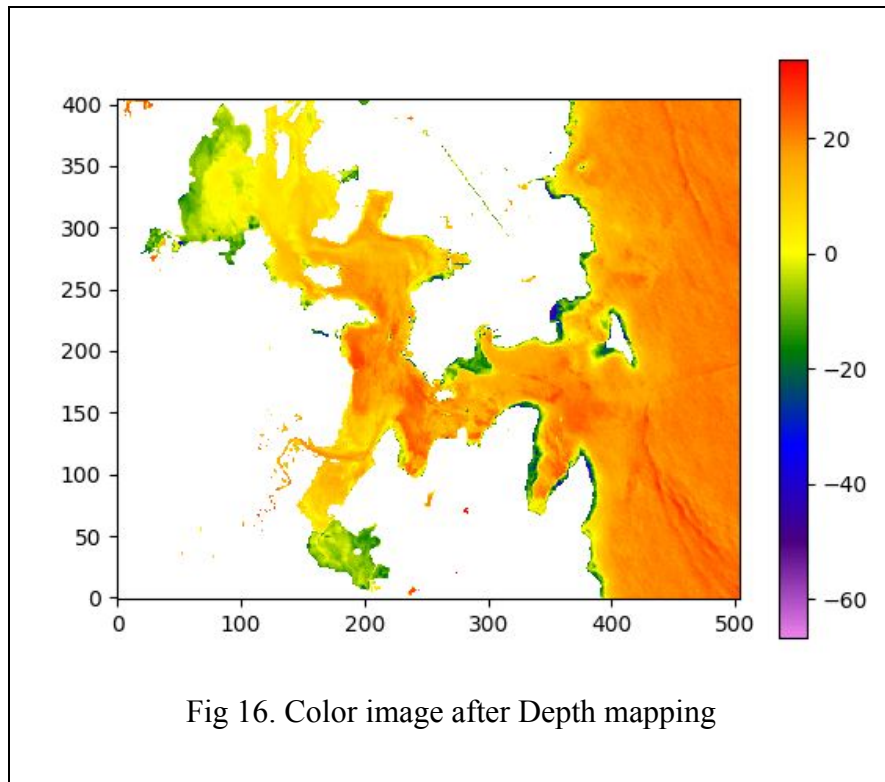
For the purposes of this report, we ran our program on ~400x500 pixel images, containing the Port Blair and Ross Island region.

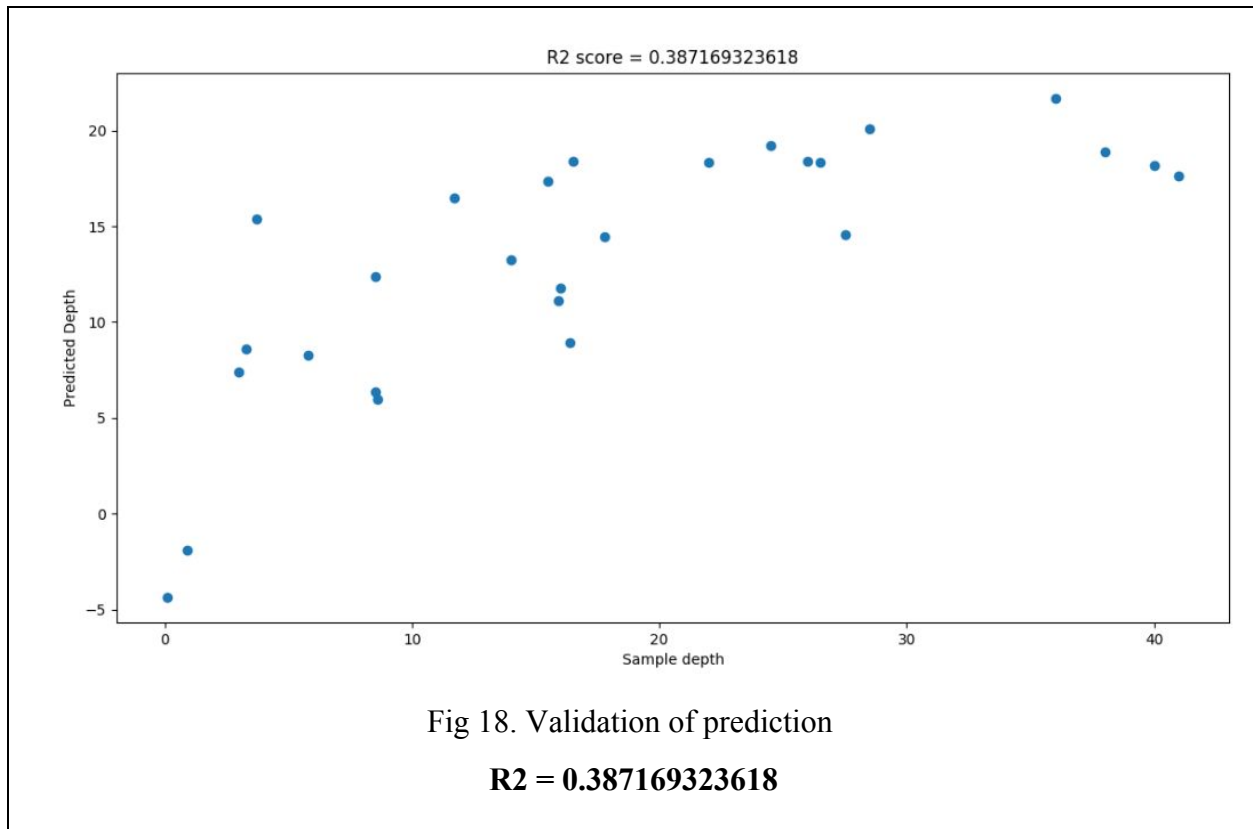
The NIR threshold value was taken to be 10000.

Following images are the result of application of water column correction:



Following images are the result of application of depth calculation:





## 9. Recommendations for future developments

LandSat 5 and LandSat 7 satellites were found to have scan line correction errors, due to which their results were not correct. Functionality can be added to clean the images of these anomalies.

Metadata processing for even more satellites may be added. For example, we looked at Sentinel-2A metadata and found it to be too vast and could not find a way to process it in our program. One may assume that the vastness of this data may add to the accuracy of mapping.

We have clearly commented the code so that anyone later might easily be able to apply a different method for depth calculation. In most cases, this will just need changing a few lines of the code.

Sub Methods for clipping Satellite Image to desired area to process, and for georeferencing the ground maps may be added within the standalone program itself instead of using QGIS.

## 10. Appendices

### Appendix - I

#### Calculation of ratio of attenuation coefficients

The gradient of the line is not calculated using conventional least squares regression analysis (which is the standard equation given by most statistical packages). This is because the result depends on which band is chosen to be the dependent variable. Therefore, rather than calculating the mean square deviation from the regression line in the direction of the dependent variable, the regression line is placed where the mean square deviation (measured perpendicular to the line) is minimised. The following equations are used.

$$\frac{k_i}{k_j} = a + \sqrt{a^2 + 1}$$

where

$$a = \frac{\sigma_{ii} - \sigma_{jj}}{2\sigma_{ij}}$$

and

$$\sigma_{ij} = \text{mean}(X_i X_j) - (\text{mean}(X_i) \times \text{mean}(X_j))$$

( $\sigma_{ii}$  is the variance of band i,  $\sigma_{ij}$  is the covariance between bands i and j)

## APPENDIX - II

### Band notations of LandSat satellites

Landsat 8 Operational Land Imager (OLI) and Thermal Infrared Sensor (TIRS)

Band	Wavelength	Useful for mapping
Band 1 – Coastal Aerosol	0.435 - 0.451	Coastal and aerosol studies
Band 2 – Blue	0.452 - 0.512	Bathymetric mapping, distinguishing soil from vegetation, and deciduous from coniferous vegetation
Band 3 - Green	0.533 - 0.590	Emphasizes peak vegetation, which is useful for assessing plant vigor
Band 4 - Red	0.636 - 0.673	Discriminates vegetation slopes
Band 5 - Near Infrared (NIR)	0.851 - 0.879	Emphasizes biomass content and shorelines
Band 6 - Short-wave Infrared (SWIR) 1	1.566 - 1.651	Discriminates moisture content of soil and vegetation; penetrates thin clouds
Band 7 - Short-wave Infrared (SWIR) 2	2.107 - 2.294	Improved moisture content of soil and vegetation and thin cloud penetration
Band 8 - Panchromatic	0.503 - 0.676	15 meter resolution, sharper image definition
Band 9 – Cirrus	1.363 - 1.384	Improved detection of cirrus cloud contamination
Band 10 – TIRS 1	10.60 – 11.19	100 meter resolution, thermal mapping and estimated soil moisture
Band 11 – TIRS 2	11.50 - 12.51	100 meter resolution, Improved thermal mapping and estimated soil moisture

Landsat 4-5 Thematic Mapper (TM) and Landsat 7 Enhanced Thematic Mapper Plus (ETM+)

Band	Wavelength	Useful for mapping
Band 1 - Blue	0.45 - 0.52	Bathymetric mapping, distinguishing soil from vegetation, and deciduous from coniferous vegetation
Band 2 - Green	0.52 - 0.60	Emphasizes peak vegetation, which is useful for assessing plant vigor
Band 3 - Red	0.63 - 0.69	Discriminates vegetation slopes
Band 4 - Near Infrared	0.77 - 0.90	Emphasizes biomass content and shorelines
Band 5 - Short-wave Infrared	1.55 - 1.75	Discriminates moisture content of soil and vegetation; penetrates thin clouds
Band 6 - Thermal Infrared	10.40 - 12.50	Thermal mapping and estimated soil moisture
Band 7 - Short-wave Infrared	2.09 - 2.35	Hydrothermally altered rocks associated with mineral deposits
Band 8 - Panchromatic (Landsat 7 only)	0.52 - 0.90	15 meter resolution, sharper image definition

## **11. References**

1. Lyzenga, David & P. Malinas, Norman & Tanis, F.J.. (2006). Multispectral bathymetry using a simple physically based algorithm. *Geoscience and Remote Sensing, IEEE Transactions on*. 44. 2251 - 2259. 10.1109/TGRS.2006.872909.
2. P, Jagalingam. (2015). Bathymetry Mapping Using Landsat 8 Satellite Imagery. *Procedia Engineering*. 116. 10.1016/j.proeng.2015.08.326.
3. Alasdair J. Edwards et al, “Remote Sensing Handbook for Tropical Coastal Management”, United Nations Educational, Scientific and Cultural Organization, 2000
4. Lyzenga, David. (1981). Remote sensing of bottom reflectance and water attenuation parameters in shallow water using aircraft and LANDSAT data. *International Journal of Remote Sensing*. 2. 71-82. 10.1080/01431168108948342.
5. ..Stumpf, R.P., Holderied, K., Sinclair, M., 2003. Determination of water depth with high-resolution satellite imagery over variable bottom types.
6. Sandwell, D.T., Gille, S.T., and W.H.F.Smith, eds., *Bathymetry from Space: Oceanography, Geophysics, and Climate*, Geoscience Professional Services, Bethesda, Maryland, June 2002, 24 pp., [www.igpp.ucsd.edu/bathymetry\\_workshop](http://www.igpp.ucsd.edu/bathymetry_workshop).

## **12. Glossary**

UTM: Universal Transverse Mercator

WGS: World Geodetic System

NIR: Near InfraRed

SWIR: Short Wave InfraRed

TIR: Thermal InfraRed

NHO: Naval Hydrographic Office